Suspended microfluidics

Benjamin P. Casavant[a,b,1], Erwin Berthier[a,b,c,1], Ashleigh B. Theberge[a,b,d,e], Jean Berthier[f], Sara I. Montanez-Sauri[a,g], Lauren L. Bischel[a,b], Kenneth Brakke[h], Curtis J. Hedman[i], Wade Bushman[a,d], Nancy P. Keller[c], and David J. Beebe[a,b,2]

[a]Carbone Cancer Center, Madison, WI 53705; Departments of [b]Biomedical Engineering, [c]Medical Microbiology and Immunology, and [d]Urology, [e]Molecular and Environmental Toxicology Center, and [g]Materials Science Program, University of Wisconsin, Madison, WI 53705; [f]Laboratoire d'Électronique des Technologies de l'Information, Commissariat à l'Energie Atomique et aux Energies Alternatives, 38054 Grenoble Cedex 9, France; [h]Susquehanna University, Selinsgrove, PA 17870; and [i]Wisconsin Clinical and Translational Research Center / Wisconsin National Primate Research Center, Madison, WI 53705

Edited by David A. Weitz, Harvard University, Cambridge, MA, and approved April 23, 2013 (received for review February 14, 2013)

Although the field of microfluidics has made significant progress in bringing new tools to address biological questions, the accessibility and adoption of microfluidics within the life sciences are still limited. Open microfluidic systems have the potential to lower the barriers to adoption, but the absence of robust design rules has hindered their use. Here, we present an open microfluidic platform, suspended microfluidics, that uses surface tension to fill and maintain a fluid in microscale structures devoid of a ceiling and floor. We developed a simple and ubiquitous model predicting fluid flow in suspended microfluidic systems and show that it encompasses many known capillary phenomena. Suspended microfluidics was used to create arrays of collagen membranes, mico Dots (μDots), in a horizontal plane separating two fluidic chambers, demonstrating a transwell platform able to discern collective or individual cellular invasion. Further, we demonstrated that μDots can also be used as a simple multiplexed 3D cellular growth platform. Using the μDot array, we probed the combined effects of soluble factors and matrix components, finding that laminin mitigates the growth suppression properties of the matrix metalloproteinase inhibitor GM6001. Based on the same fluidic principles, we created a suspended microfluidic metabolite extraction platform using a multilayer biphasic system that leverages the accessibility of open microchannels to retrieve steroids and other metabolites readily from cell culture. Suspended microfluidics brings the high degree of fluidic control and unique functionality of closed microfluidics into the highly accessible and robust platform of open microfluidics.

high throughput metabolomics | multiplexed cell culture | spontaneous capillary flow | passive biphasic systems | arrayed migration platform

Open microfluidic systems offer unique advantages, creating platforms that provide increased accessibility, robustness, functionality, and simplicity of fabrication. An inherent feature of these systems is the introduction of an air–liquid interface (1), a component that makes understanding and characterizing fluid flows in these systems complex. However, these phase interfaces can be leveraged to provide unique functionality, integrating the enabling features of phase interfaces demonstrated in closed systems while maintaining the benefits of the open systems. Air–liquid and liquid–liquid phase interfaces in closed systems [reviewed by Atencia and Beebe (2)] have been demonstrated for ultrahigh-throughput screening (3), protein purification (4), organ models (5), cell invasion assays (6), and small-molecule extraction (7). These closed microfluidic approaches often use pinning to create a vertical interface between a series of pillars or ridges (8–11), or require the use of tubes and actuation devices (12–14). Although open systems provide a significantly different approach to interfacing with microscale devices (15–18), the lack of control over the fluid flow prevents the development of platforms with the complexity and functionality necessary for many applications (19). Recently demonstrated open microfluidic platforms have yielded systems with unique functionality through connected microfluidic cell cultures to protein detection platforms (20), neutrophil migration platforms (21), or single-cell actuation devices (15). The need for control within these platforms is paramount, with studies evaluating the robustness of fluid handling within open devices (22, 23), but these open devices have still been limited to methods that rely on active pumping or patterning methods and are difficult to fabricate and operate. Interestingly, Melin et al. (23) demonstrated a closed microfluidic system that was directly interfaced with an open system to leverage benefits of both to build complexity into accessible and reliable open microfluidic systems.

Here, we develop an encompassing concept for microscale capillary flow, called suspended microfluidics, that enables a high degree of control for channels operating with multiple air or immiscible fluidic interfaces. In these systems, fluid flow occurs in an open microchannel, such that the fluid is "suspended" between two or more air environments or between air and a second immiscible liquid. The phenomenon relies on the generation of spontaneous capillary flow (SCF) in a channel that has neither a ceiling nor a floor (Fig. 1 *A–D*). In the channel, the fluid front advances (defined as SCF occurring) when the energy reduction associated with the larger liquid–solid surface area outweighs the energy increase associated with the larger liquid–air interface area. Suspended microfluidics is a robust and accessible class of microscale capillary flow that allows the creation of horizontal phase interfaces in open microfluidic systems. The platform technology developed here enables accessible, multiplexed systems for biochemical and cell-based assays and can impart unique functionality to microfluidic assays. Importantly, SCF can be used for many fluids with properties including aqueous solutions, hydrogels, oils, and organic immiscible solvents, and in a wide range of open geometries. This makes suspended microfluidics well suited for a large scope of applications, and to highlight this aspect, we demonstrate here the ability to create (*i*) a highly multiplexed 3D biochemical assay for tumor cell response, (*ii*) horizontal microtranswells for cellular invasion assays, and (*iii*) a microscale culture and solvent extraction platform for metabolomics assays.

Results and Discussion

Modeling SCF. To determine geometrical considerations that allow the robust design of channels enabling SCF, we developed an analytical model in which a fluid flows in a channel containing open air–liquid interfaces without external pressure applied to initiate flow. At each point down the length of the channel, the cross-section can be defined with sections of solid wall, which

Author contributions: B.P.C., E.B., A.B.T., J.B., S.I.M.-S., L.L.B., W.B., N.P.K., and D.J.B. designed research; B.P.C., E.B., A.B.T., J.B., S.I.M.-S., L.L.B., K.B., and C.J.H. performed research; B.P.C., E.B., A.B.T., J.B., S.I.M.-S., L.L.B., K.B., and C.J.H. contributed new reagents/analytic tools; B.P.C., E.B., A.B.T., J.B., S.I.M.-S., L.L.B., K.B., and C.J.H. analyzed data; and B.P.C., E.B., A.B.T., and D.J.B. wrote the paper.

Conflict of interest statement: B.P.C. and E.B. have ownership in Tasso, Inc. D.J.B. has ownership in Bellbrook Labs LLC; Ratio, Inc.; and Salus Discovery LLC.

This article is a PNAS Direct Submission.

Freely available online through the PNAS open access option.

[1]B.P.C. and E.B. contributed equally to this work.

[2]To whom correspondence should be addressed. E-mail: djbeebe@wisc.edu.

This article contains supporting information online at www.pnas.org/lookup/suppl/doi:10.1073/pnas.1302566110/-/DCSupplemental.

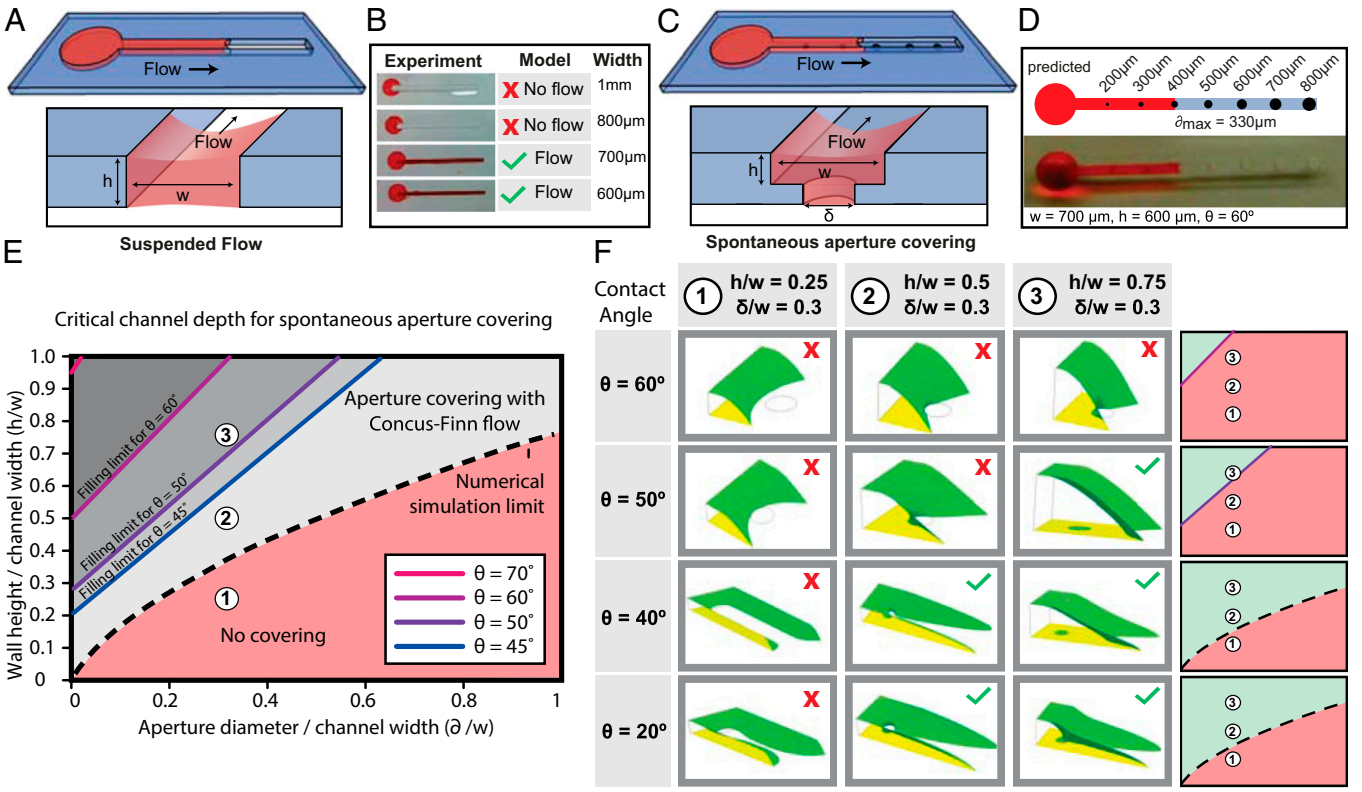

Fig. 1. SCF describes fluid flow in a channel devoid of a ceiling or a floor. Suspended microfluidic channel with height (h) and width (w) that is open on the top and bottom surfaces can enable flow (*A*) as predicted by the analytical model and validated by experiment (*B*). Apertures (with diameter δ) in the floor of a U-shaped channel create individual suspended membranes (*C*) with experimental validation demonstrating the limit to aperture filling (*D*). (*E* and *F*) Analytical model describes flow at various contact angles. (*E*) Solid lines represent the boundary between filling (above the line) and nonfilling (below the line) for individual contact angles greater than the Concus–Finn limit, and the dashed line represents the boundary between filling (above the line) and nonfilling (below the line) for all contact angles less than the Concus–Finn limit. (*F*) Surface Evolver simulations validate the analytical model for three different channel geometries.

define the wetted perimeter (p_w), and free air–liquid interface (p_f), which defines the free perimeter. Using a quasi–steady-state surface energy analysis, we derived a ubiquitous condition for SCF, given a fluid of contact angle θ that remains valid for most open and suspended microchannels (Eq. **1** and Fig. S1):

$$\frac{p_f}{p_w} < cos(\theta) \qquad [1]$$

We first validated the analytical model given in Eq. **1** using a suspended channel composed of two sides and lacking both a floor and a ceiling. In this embodiment, the equation for SCF becomes $w/h < cos(\theta)$, where w and h are the width and height of the channel, respectively, and we find that the experimental results, analytical model, and numerical simulations using Surface Evolver software (www.susqu.edu/brakke/evolver/evolver.html) correspond closely (Fig. 1 *A* and *B* and Fig. S2). To create multiple isolated suspended interfaces in the same channel, we created a microchannel with a U-shaped cross-section containing circular apertures in the floor (Fig. 1*C*). For this geometry, an SCF condition featuring the aperture diameter δ can be determined from Eq. **1** (Fig. S2). Although Eq. **1** predicts SCF accurately for fluids with higher contact angles (Fig. 1*D* and Fig. S3), the advancement of the fluid front is more complex for fluids with contact angles lower than the Concus–Finn limit, a condition dictating whether fluid can flow as a filament in a wedge (24). In this case, the fluid separates into two filaments on each side of the aperture, and SCF can still occur if these filaments merge and fill the aperture (Fig. S3). We have developed algorithms using Surface Evolver to establish more inclusive design criteria (Fig. 1 *E* and *F* and Fig. S3). Beyond the two suspended microfluidic geometries described here, the model defined by Eq. **1** provides a reliable design rule to create open and suspended microfluidic channels allowing SCF for most geometries. More generally, we find that Eq. **1** also predicts many capillary phenomena, such as capillary flow in a tube or the condition for Concus–Finn filament

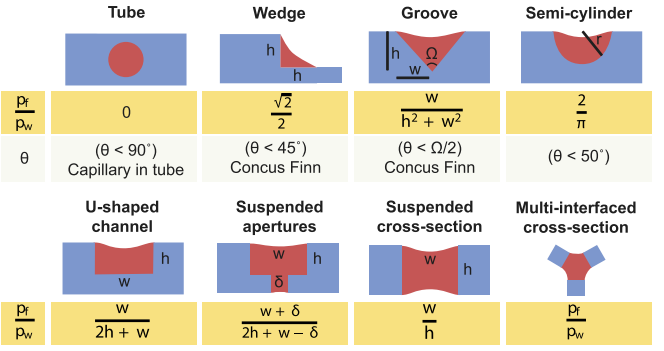

Fig. 2. Calculation of the SCF criterion for different geometries. Eq. **1** remains valid for many current known models, such as capillary flow in a tube and Concus–Finn flow in a wedge or groove, in addition to predicting flow in previously undescribed suspended systems. p_f, perimeter of free (unbounded) surfaces; p_w, perimeter of wetted surfaces at the cross-sectional plane of the channel at the fluid front.

growth (Fig. 2 and Figs. S4 and S5), establishing it as a global model for capillary phenomena.

Multiplexed 3D Culture Screening Platform. The emerging importance of the cellular microenvironment requires new tools to enable quantitative manipulation of microenvironmental parameters, including chemical and biological composition. We leveraged the ability of SCF to flow hydrogels in channels containing apertures in the floor to create nanoliter deposits of hydrogels. The resulting hydrogel membranes, or μDots, are suspended between a top open microfluidic channel and a bottom microchannel, creating a high-density array for parametric multiplexing that can be filled and used with a pipette (Fig. 3 *A* and *B*). The design of the μDots involved a top U-shaped channel with apertures in the floor, such that the apertures connected with a channel in a second layer of channels below. Using a series of U-shaped channels in a top layer of polydimethylsiloxane (PDMS) and a series of channels in a bottom layer of PDMS perpendicular to the top channels, we created an array of apertures, each accessible from the top by one channel and from the bottom by another channel (Fig. 3*C*). We thus demonstrate an ultrasimple multiplexing platform in which each assaying point is individually addressable and that does not require a valving or pneumatic control layer. We created the μDots in the apertures by pipetting, aspirating, and polymerizing a plug of gel in them. To demonstrate the robustness and multiplexing potential of μDots, a 4 × 10 (40-μDot) array was created using the same workflow (Fig. 3*D*). Nanoliter volumes of gel were suspended and polymerized in the μDots, allowing control over soluble factors and chemical compositions of the microenvironments. Using this platform, a high experimental density can be achieved in a compact device footprint, enabling an efficient analysis of cellular phenomena in response to combinations of factors found within the cellular microenvironment (Fig. 3 *E–G* and Fig. S6).

To demonstrate the multiplexing potential of μDots for studying regulation of cancer cell proliferation, we performed an experiment to explore the interaction of extracellular matrix (ECM) components with soluble treatments (e.g., inhibitors, growth factors). We embedded breast cancer (T47D) cells in μDots with various ECM compositions on each row of the multiplexing platform and applied a set of soluble treatments in medium in each column (Fig. 3*F*). We evaluated the average cell cluster size after 4 d of culture in 3D conditions and found that a broad-spectrum matrix metalloproteinase (MMP) inhibitor, GM6001 (Millipore), affected cluster growth as expected. However, in laminin- or fibronectin-rich ECM compositions, the MMP inhibitor displayed a marked decrease in action, as evidenced by larger cluster sizes, demonstrating that these chemical

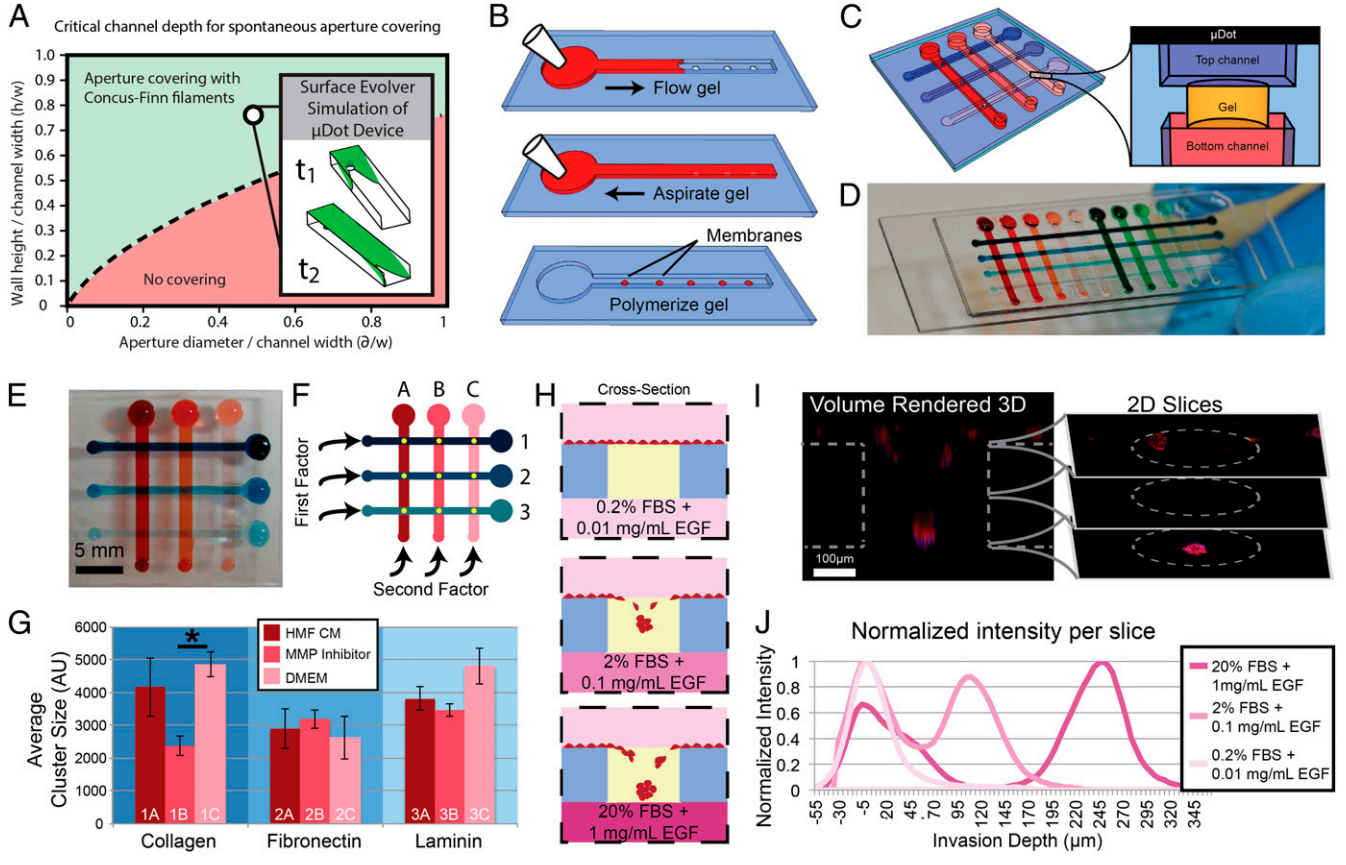

Fig. 3. Suspended microfluidic multiplexed screening array using a μDot device. (*A*) μDot device geometrical parameters are indicated with an open circle on the plot of parameter space. (*Inset*) Surface Evolver simulation at two stages of the simulation. (*B*) Creation of μDots requires a three-step process of *i*) filling, and *ii*) aspirating a hydrogel, followed by *iii*) a polymerization step. (*C*) Schematic of the gel μDot array accessible from above and below. (*D*) 4 × 10 array of μDots. (*E* and *F*) 3 × 3 array used to screen the response of breast cancer (T47D) cells to many combinatorial factors. (*G*) Cells were exposed to *i*) conditioned medium (CM) from human mammary fibroblast (HMF) culture (HMF CM), *ii*) MMP inhibitor added to HMF CM (MMP Inhibitor), or *iii*) standard Dulbecco's Modified Eagle's Medium (DMEM) within three different ECM conditions: collagen, fibronectin, and laminin created a 9-parameter array. A significant difference in average cluster size after 4 of culture was found between MMP inhibitor and DMEM in collagen ECM (*$P < 0.05$, n = 3). Error bars are SD. AU, arbitrary units. (*H–J*) Invasion assay to assess the invasion of prostate cancer (PC3-MM2) cells toward various chemoattractants. A schematic (*H*) illustrates the data obtained in a confocal image (*I*) that can be used by slice to evaluate invasion depth (*J*) ($n = 48$ cells).

treatments were highly sensitive to ECM composition, a factor that should be strongly considered when testing potential anticancer drugs (25) (Fig. 3*G*). To achieve comparable levels of multiplexing using traditional closed microfluidic systems would require complex valving, fabrication, and control systems for high-throughput screening arrays. The benefits of SCF yield open systems that simultaneously provide control over the fluid flow of traditional closed systems and the experimental simplicity and density of open microwell approaches. This unique combination resulted in a platform that is capable of exploring a wide range of factors found in the cellular microenvironment critical to understanding the complexities of cancer regulation and progression.

A Cellular Invasion Platform. Virtual membranes created by SCF in the μDot array also enable a unique membrane-free cell invasion assay inspired by the macroscopic gold-standard transwell platform. We demonstrate this application with an assay designed for studying the collective invasion of prostate cancer (PC3-MM2) cells through a 3D ECM (Matrigel; BD Biosciences). We introduced a range of chemoattractants in the medium below the matrix by adding varying amounts of fetal bovine serum (FBS) and epidermal growth factor (EGF) into the bottom channels (Fig. 3*H*). Confocal imaging was used to track the extent of cellular invasion after 24 h in culture (Fig. 3*I*). We observed that cells placed on the opposite side of a high chemoattractant concentration migrated the farthest into the gel, whereas cells seeded on gel above control medium without chemoattractant did not display noticeable invasion (Fig. 3*J*). Importantly, the horizontal configuration of the μDots enabled us to discern the collective invasion of the group of cells, because each cell is placed at the same "starting line" and exposed to the same gradient of chemoattractant. This phenomenon displays interesting readout ability because all the cells can invade together toward a chemoattractant source in a parallel plane to the starting position of the cells, as opposed to being disseminated migrating toward an in-plane chemoattractant source as most in vitro invasion assays necessitate. The μDot embodiment of the transwell enables high-density invasion assays using a passive multiplexing method, allowing a simple approach to explore large-parameter spaces (e.g., screening assays) for a functional cellular end point.

Biphasic Metabolomic Platform. SCF is a ubiquitous method for generating flow in both open systems containing air–liquid interfaces, as described previously, and immiscible liquid interfaces. We demonstrated the ability to flow an immiscible organic solvent in a suspended microfluidic system over an aqueous solution, allowing the creation of open, passive, and static biphasic platforms. This enabling property was used to develop a microsystem for the extraction of small molecules secreted by cells in culture into organic solvents to perform metabolomic studies. We confirmed that the same equation describing the flow of aqueous fluid in an open microchannel could be applied to organic solvent flowing in an open U-shaped channel with apertures in the floor (Fig. 4*A*). Specifically, we flowed pentanol in a U-shaped channel containing an array of apertures in the floor, creating contact between the pentanol and aqueous medi from mammalian cell culture in a channel below (Fig. 4 *B* and *C*). This fluidic connection allows the diffusion of specific small-molecule metabolites from the aqueous phase to the organic phase. Here, we highlight the utility of this platform in a proof-of-concept experiment in which we studied adrenal cell steroidogenesis and chose pentanol to extract steroids with ranging polarities.

The study of steroidogenesis has become an important area of research in human development and molecular toxicology. It is a critical driver of normal development, and aberrant steroidogenesis can occur in response to in utero toxicant exposure, resulting in birth defects (26). Likewise, steroidogenic pathways are hijacked in late-stage prostate cancer, significantly contributing to mortality (27). To understand and develop treatments for aberrant steroidogenesis better, as well as to identify environmental toxicants that may disrupt normal steroidogenesis, more advanced in vitro techniques are required. The reduced culture volumes inherent to microfluidic cell culture models enable the ability to work with limited primary cell samples, such as cells from biopsies in patients with prostate cancer and in fetal rodent models, and the technique presented herein streamlines analysis by incorporating on-chip isolation of steroids for downstream

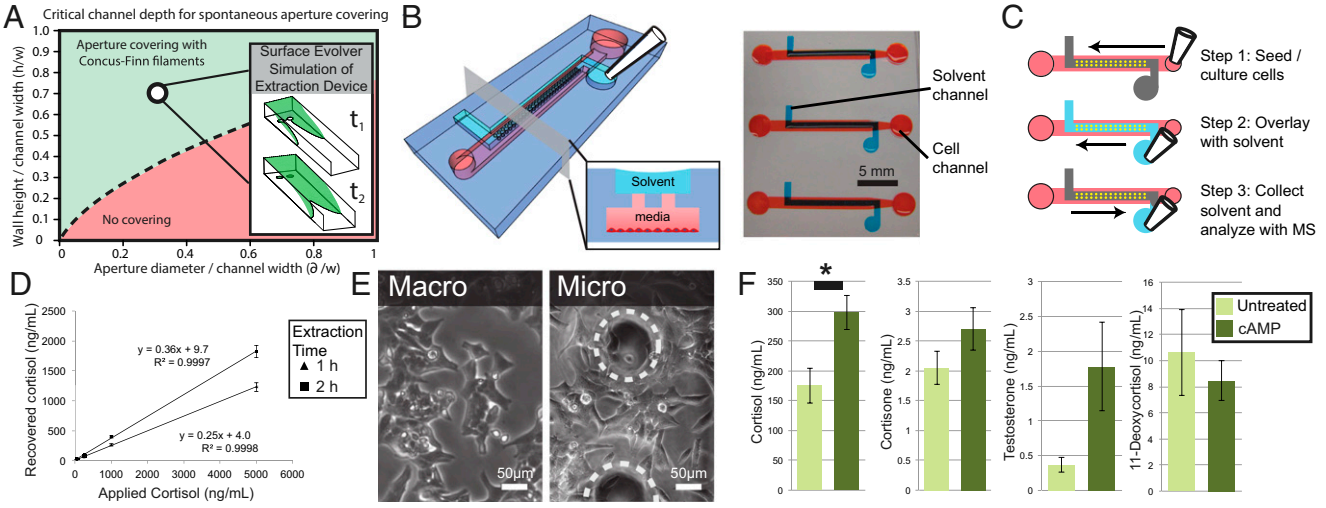

Fig. 4. Suspended microfluidics for solvent extraction of small molecules. (*A*) Extraction device geometrical parameters are indicated with an open circle on the plot of parameter space. (*Inset*) Surface Evolver simulation at two stages of the simulation. Schematic of the device illustrates the solvent channel overlaid on a cell culture channel with apertures connecting the two (*B*) with the device operation shown (*C*). (*D*) Standard curve shows robust steroid retrieval over a range of cortisol levels from 50 to 5,000 ng/mL with 24 ± 1% recovery for a 1-h extraction and 38 ± 1% recovery for a 2-h extraction ($n = 5$). Error bars represent SE. (*E* and *F*) Solvent extraction of steroids from cell culture medium. (*E*) Adrenal (NCI-H295A) cells within the device (micro) display a similar morphology to those cultured in a six-well plate (macro). Dotted circles outline extraction apertures. (*F*) Steroids extracted from microfluidic cell culture. Cortisol production increased significantly (*$P < 0.05$) with 8Br-cAMP (0.5 mM) treatment ($n = 3$). Error bars represent SE.

quantification using liquid chromatography-mass spectrometry (LC-MS). To validate the approach, cortisol solutions of known concentration were extracted with pentanol on chip, demonstrating consistent extraction over a range of biologically relevant cortisol concentrations (Fig. 4*D*). The microscale extraction platform also demonstrated extraction efficiencies 24 ± 1% and 38 ± 1% for 1-h and 2-h extractions, respectively, suggesting that diffusion at the microscale allows extraction efficiencies that are more than sufficient for downstream LC-MS detection and that the vigorous agitation typically used to mix the aqueous and organic phase in macroscale extractions is not necessary on the microscale level. We cultured the adrenocortical cell line NCI-H295A within the microchannels (Fig. 4*E*) and used integrated microfluidic extraction to isolate a panel of steroids from the cell culture medium at the end of the culture period. The cells produced detectable levels of steroids under microculture conditions. Furthermore, to demonstrate the potential of this technique for evaluating the effects of drugs or toxicants on steroidogenesis, we applied a known stimulant of steroidogenesis, 8-bromoadenosine 3′,5′-cyclic monophosphate (8Br-cAMP). As expected, cortisol production significantly increased in response to 8Br-cAMP, further validating the platform for microfluidic steroidogenesis assays (Fig. 4*F*).

Traditional methods for extraction of steroids and, more generally, metabolites require many manual steps to mix and separate the organic and aqueous layers. In contrast, suspended microfluidics allows a tubeless, passive, and accessible approach to create biphasic flows in microdevices, which can easily be arrayed and interfaced with a multichannel pipette or automated liquid handler for high-throughput applications. A prime application for this platform is the screening for toxicants that contribute to birth defects by disrupting steroidogenesis in utero or for drugs that prevent steroidogenesis in late-stage prostate cancer. In addition to studying known analytes, such as steroids, this technology can be used to discover new metabolites and metabolic profiles in mammalian, fungal, or bacterial cultures. Discovery studies will be aided by the ability to work with a large range of solvents. In particular, low-volatility solvents that are prohibitively hard to evaporate when working with milliliter quantities can be evaporated without additional equipment and more efficiently when microliter quantities are used. Further, capitalizing on surface tension, this platform ensures that the solvent phase is always accessible in the upper channel regardless of density, and inseparable emulsions that sometimes occur due to agitation in macroscale extractions are avoided altogether.

Conclusions

The ability to generate SCF in an open microfluidic channel enables the creation of suspended microfluidic flows vertically separating two liquid or gaseous environments in a simple, robust, and precise way. The analytical model developed in Eq. **1** provides a ubiquitous method to design suspended microfluidic systems that allow SCF to occur in any user-designed geometries, merging the precision fluidic control and unique functionality of closed microfluidics with the highly accessible and robust platform of open microfluidics. This simple equation guides the creation of a unique class of devices that leverage open interfaces tailored to specific applications. Using suspended microfluidics, we created arrays of μDots and applied them to questions of cell invasion and cell growth. We used the device to discern collective and individual cell invasion toward a source chemoattractant. Suspended microfluidics allowed for the creation of simple and robust high-throughput multiplexed screening arrays to study cell growth within 3D matrices. Finally, with the same suspended microfluidic principles, biphasic systems can be created and controlled to extract metabolites from microfluidic systems, greatly simplifying solvent extraction on the microscale with utility toward cancer biology and fungal and bacterial metabolite screening and discovery assays. The diversity of the three applications demonstrated in this paper speaks to the broad applicability of suspended microfluidics, because the demonstrated techniques only explore a small range of the potential configurations allowed using this approach. Suspended microfluidics presents a unique technological paradigm for functionality in biological investigations.

Materials and Methods

Numerical Simulations. We used Surface Evolver software (28) to perform numerical simulations on the advancement or stalling of the liquid front in suspended microfluidic configurations. We determined the conditions for which SCF was impossible when an energetic-equilibrium point could be found. When the software was not able to determine an equilibration point, we considered that SCF was possible. Two Surface Evolver scripts were developed to solve the problems of mesh sizes increasing too fast in the corners of the U-groove and of numerical errors at the advancing triple line over an aperture.

Mold and Microdevice Fabrication. We fabricated the microchannels in PDMS (Sylgard; Dow Corning) molded from a silicon-SU8 mold. Through-holes in the PDMS layer were incorporated into the mold and achieved by applying weight on top of the PDMS during the curing process. PDMS channels used for solvent extraction experiments were coated with 15 μm of parylene C (PD2010; SCS). Channels were plasma-treated after parylene coating to achieve a contact angle ranging from 20° to 30°.

SCF. PDMS channels containing apertures in the floor of the channel were designed at a constant height of 700 μm and a width of 800 μm, with apertures increasing in size from 200 to 800 μm over the course of the channel. To render the surfaces hydrophilic, the devices were subjected to oxygen plasma treatment. A red aqueous dye (Allura Red) mixed 1:1 with deionized water was added to the device to characterize the SCF.

μDot Array for Parametric Multiplexing. PDMS channels for μDot arrays were created using two molded layers: a top layer of a U-shaped microfluidic device with apertures in the floor and a bottom layer of U-shaped channels. To prepare a μDot device, the individual PDMS devices were fabricated using standard soft lithography techniques as detailed in *SI Materials and Methods* and plasma-treated to achieve a contact angle ranging from 15° to 30°. When using PDMS-based devices, plasma treatment must be applied immediately before use due to variations in the contact angle resulting from hydrophobic recovery; however, the use of hard thermoplastics allows longer storage times between plasma treatment and use. Devices were bonded by placing the upper PDMS device on the lower PDMS U-shaped device, such that each aperture was addressed by a top channel and a lower channel. This combined device was placed onto any convenient holder, either a glass slide or a Nunc Omnitray (Thermo Fisher Scientific), for device portability, because devices were entirely self-enclosed. Matrigel solutions were then flowed by pipette in the U-shaped top channel of the μDot array and were able to flow over and into the aperture by means of SCF. We subsequently removed the gel from the channels by aspirating the excess, leaving suspended gels in each of the through-holes. Gels were polymerized by placing the entire device in an incubator at 37 °C for 10 min.

Cell Culture. The T47D breast carcinoma cell line and NCI-H295A adrenocortical cell line were generously donated by M. Gould (University of Wisconsin) and by the laboratory of G. D. Hammer (University of Michigan, Ann Arbor, MI) (29), respectively. All cells were maintained in standard culture flasks before seeding into microchannels.

Steroid Extraction from Microculture on Chip. NCI-H295A cells were suspended in cell culture medium with or without 0.5 mM 8Br-cAMP (Sigma–Aldrich) and seeded in the bottom channel of each microfluidic device. After 48 h in culture, steroids were extracted from cell culture medium by adding 1-pentanol (Sigma–Aldrich) to the top channel of the microfluidic device as detailed in *SI Materials and Methods*. This experiment was performed three times with two to four replicates within each experiment.

Extraction of Cortisol Standard Solutions on Chip. Cortisol standard solutions were prepared in medi used for the NCI-H295A cell culture with 0.1% methanol at the following concentrations: 50, 250, 1,000, and 5,000 ng/mL. Cortisol solution was added to the bottom channel of the microfluidic device, and samples were extracted for a total of 1 h and 2 h as described in *SI Materials and Methods*. This experiment was performed using five microfluidic channels for each cortisol concentration.

HPLC-MS/MS Analysis of Pentanol Microfluidic Channel Extracts for Hormones. Microfluidic channel pentanol extracts were reduced to dryness and reconstituted in a water/methanol solution (80:20 vol/vol). Hormone analysis was performed using an integrated HPLC system (Prominence UFLC XR; Shimadzu) coupled to a quadrupole-linear ion trap mass spectrometer (QTRAP 5500 MS/MS; AB/SCIEX) operating with atmospheric pressure chemical ionization in positive ionization mode (Tables S1 and S2).

Confocal Microscopy. We prepared a red cell-tracker dye solution (Invitrogen) in PBS, flowed it in the top and bottom channels of the μDot array, and incubated the device for 30 min. After washing with PBS, we fixed, permeabilized, and stained the cells using a DAPI stain. We imaged the device on a Digital Eclipse C1 Plus confocal microscope (Nikon) with a slice height of 5 μm. We created final rendered images using the freeware OsiriX.

Multiplexing the Effect of ECM Components, Soluble Factors, and MMP Inhibitors in T47D Cell Growth. A stock collagen type I solution (rat tail; BD Biosciences) with Hepes buffer was prepared. Cells were trypsinized and resuspended in serum-free (SF) medium. FBS and T47D cells were added to the collagen gels, and SF media was used to adjust the final concentrations to 5×10^5 cells/mL, 4% (vol/vol) FBS, and 3.0 mg/mL collagen. For experiments that included fibronectin or laminin, either fibronectin (1 mg/mL, human; BD Biosciences) or laminin (1.88 mg/mL, mouse; BD Biosciences) was introduced into the collagen gels at a concentration of 100 μg/mL. Gels containing T47D cells were loaded on the bottom channels of the μDot arrays and incubated for 10 min for polymerization. Human mammary fibroblast (HMF) CM was collected from a 2-d culture of HMFs. A broad-spectrum MMP inhibitor (GM6001) was diluted to 5 μM using SF medi, mixed with HMF CM to a get final GM6001 concentration of 500 nM, and mixed with 25% (vol/vol) fresh medium. Fresh medium was used as a control. All soluble formulations (HMF CM, MMP inhibitor medium, and medium) were added through the top channels of the μDots arrays and changed every other day for 7 d.

ACKNOWLEDGMENTS. We thank Jay Warrick and Edmond Young for assistance in designing the μDot device, Eric Sackmann for access to specific reagents, and Lloyd Smith and Mark Scalf for preliminary LC-MS analyses. B.P.C. and D.J.B. were supported by a Department of Defence Prostate Cancer Research Program (PCRP) award (Grant W81XWH-09-1-0192), N.P.K. and E.B. were supported by the National Science Foundation- Emerging Frontiers in Research and Innovation-MIKS (Grant 1136903) and by a grant from the American Asthma Foundation, and A.B.T. was supported by the National Institutes of Health (NIH) (Grant T32ES007015). D.J.B was supported by NIH Grants R01 EB010039 and R33 CA137673. LC-MS performed in this study was supported by the Institute for Clinical and Translational Research core laboratory (NIH Grant 1UL1RR025011) and by NIH Grant P51OD011106/P51RR000167. L.L.B. was supported by NIH Grant T32HL007889. S.I.M.-S. was supported by NIH Grant T32GM08349.

1. Zhao B, Moore JS, Beebe DJ (2001) Surface-directed liquid flow inside microchannels. *Science* 291(5506):1023–1026.
2. Atencia J, Beebe DJ (2005) Controlled microfluidic interfaces. *Nature* 437(7059):648–655.
3. Agresti JJ, et al. (2010) Ultrahigh-throughput screening in drop-based microfluidics for directed evolution. *Proc Natl Acad Sci USA* 107(9):4004–4009.
4. Berry SM, Alarid ET, Beebe DJ (2011) One-step purification of nucleic acid for gene expression analysis via Immiscible Filtration Assisted by Surface Tension (IFAST). *Lab Chip* 11(10):1747–1753.
5. Huh D, et al. (2010) Reconstituting organ-level lung functions on a chip. *Science* 328 (5986):1662–1668.
6. Repesh LA (1989) A new in vitro assay for quantitating tumor cell invasion. *Invasion Metastasis* 9(3):192–208.
7. Mary P, Studer V, Tabeling P (2008) Microfluidic droplet-based liquid-liquid extraction. *Anal Chem* 80(8):2680–2687.
8. Beebe DJ, et al. (2000) Functional hydrogel structures for autonomous flow control inside microfluidic channels. *Nature* 404(6778):588–590.
9. Song S, Singh AK, Shepodd TJ, Kirby BJ (2004) Microchip dialysis of proteins using in situ photopatterned nanoporous polymer membranes. *Anal Chem* 76(8):2367–2373.
10. Berthier J, et al. (2009) On the pinning of interfaces on micropillar edges. *J Colloid Interface Sci* 338(1):296–303.
11. Lee SH, et al. (2010) Capillary based patterning of cellular communities in laterally open channels. *Anal Chem* 82(7):2900–2906.
12. Wong AP, Perez-Castillejos R, Christopher Love J, Whitesides GM (2008) Partitioning microfluidic channels with hydrogel to construct tunable 3-D cellular microenvironments. *Biomaterials* 29(12):1853–1861.
13. Hong JW, Quake SR (2003) Integrated nanoliter systems. *Nat Biotechnol* 21(10):1179–1183.
14. Paguirigan AL, Beebe DJ (2008) Microfluidics meet cell biology: Bridging the gap by validation and application of microscale techniques for cell biological assays. *Bioessays* 30(9):811–821.
15. Hsu C-H, Chen C, Folch A (2004) "Microcanals" for micropipette access to single cells in microfluidic environments. *Lab Chip* 4(5):420–424.
16. Olofsson J, et al. (2004) A microfluidics approach to the problem of creating separate solution environments accessible from macroscopic volumes. *Anal Chem* 76(17):4968–4976.
17. Gau H, Herminghaus S, Lenz P, Lipowsky R (1999) Liquid morphologies on structured surfaces: from microchannels to microchips. *Science* 283(5398):46–49.
18. Seemann R, Brinkmann M, Kramer EJ, Lange FF, Lipowsky R (2005) Wetting morphologies at microstructured surfaces. *Proc Natl Acad Sci USA* 102(6):1848–1852.
19. Fernandes TG, Diogo MM, Clark DS, Dordick JS, Cabral JMS (2009) High-throughput cellular microarray platforms: applications in drug discovery, toxicology and stem cell research. *Trends Biotechnol* 27(6):342–349.
20. Sardesai NP, Kadimisetty K, Faria R, Rusling JF (2013) A microfluidic electrochemiluminescent device for detecting cancer biomarker proteins. *Anal Bioanal Chem* 405(11):3831–3838.
21. Keenan TM, Frevert CW, Wu A, Wong V, Folch A (2010) A new method for studying gradient-induced neutrophil desensitization based on an open microfluidic chamber. *Lab Chip* 10(1):116–122.
22. Oliveira NM, Neto AI, Song W, Mano JF (2010) Two-dimensional open microfluidic devices by tuning the wettability on patterned superhydrophobic polymeric surface. *Appl Phys Express* 3:085205.
23. Melin J, van der Wijngaart W, Stemme G (2005) Behaviour and design considerations for continuous flow closed-open-closed liquid microchannels. *Lab Chip* 5(6):682–686.
24. Concus P, Finn R (1969) On the behavior of a capillary surface in a wedge. *Proc Natl Acad Sci USA* 63(2):292–299.
25. Weigelt B, Lo AT, Park CC, Gray JW, Bissell MJ (2010) HER2 signaling pathway activation and response of breast cancer cells to HER2-targeting agents is dependent strongly on the 3D microenvironment. *Breast Cancer Res Treat* 122(1):35–43.
26. Scott HM, Mason JI, Sharpe RM (2009) Steroidogenesis in the fetal testis and its susceptibility to disruption by exogenous compounds. *Endocr Rev* 30(7):883–925.
27. Locke JA, et al. (2008) Androgen levels increase by intratumoral de novo steroidogenesis during progression of castration-resistant prostate cancer. *Cancer Res* 68(15):6407–6415.
28. Brakke KA (1992) The Surface Evolver. *Exp Mat* 1:141–165.
29. Babu PS, Bavers DL, Shah S, Hammer GD (2000) Role of phosphorylation, gene dosage and Dax-1 in SF-1 mediated steroidogenesis. *Endocr Res* 26(4):985–994.